EUROPHYSICS LETTERS 15 August 2005

Europhys. Lett., **71** (4), pp. 651–657 (2005)
DOI: 10.1209/epl/i2005-10130-3

Scaling and hydrodynamic effects in lamellar ordering

Aiguo Xu[1](*), G. Gonnella[1], A. Lamura[2], G. Amati[3] and F. Massaioli[3]

[1] *Dipartimento di Fisica, Università di Bari and Center of Innovative Technologies for Signal Detection and Processing (TIRES) and INFN, Sezione di Bari and INFM via Amendola 173, 70126 Bari, Italy*
[2] *Istituto Applicazioni Calcolo, CNR, Sezione di Bari via Amendola 122/D, 70126 Bari, Italy*
[3] *CASPUR - via dei Tizii 6/b, 00185 Roma, Italy*

received 7 February 2005; accepted in final form 23 June 2005
published online 20 July 2005

PACS. 64.75.+g – Solubility, segregation, and mixing; phase separation.
PACS. 05.70.Ln – Nonequilibrium and irreversible thermodynamics.
PACS. 47.20.Hw – Morphological instability; phase changes.

Abstract. – We study the kinetics of domain growth of fluid mixtures quenched from a disordered to a lamellar phase. At low viscosities, in two dimensions, when hydrodynamic modes become important, dynamical scaling is verified in the form $C(\boldsymbol{k},t) \sim L^{\alpha} f[(k-k_M)L]$, where C is the structure factor with maximum at k_M and L is a typical length with logarithmic growth at late times. The presence of extended defects can explain the behavior of L. Three-dimensional simulations confirm that diffuse grain boundaries inhibit complete ordering of lamellae. Applied shear flow alleviates frustration and gives power law growth at all times.

Introduction. – The kinetics of the growth of ordered phases after a quench from a disordered state continues to provide interesting physical questions. While the process is reasonably well understood for the case of binary mixtures, where dynamical scaling occurs and domains grow with power law behavior [1], basic questions remain to be clarified for more complex systems [2]. In this letter, we consider the case of fluid mixtures where, due to competing interactions, the system would arrange itself in stripes. Examples are di-block copolymer melts, where chains of type A and B bonded in pairs, segregate at low temperatures in regions separated by a stack of lamellae [3], or ternary mixtures where surfactant form interfaces between oil and water [4]. Other systems with lamellar order are smectic liquid crystals [5], dipolar [6] and supercooled liquids [7], chemically reactive binary mixtures [8]. Lamellar patterns are also observed in Raleigh-Bénard cells above the convective threshold [9].

The ordering of lamellar systems is characterized by the presence of frustration on large scales. This affects the late time evolution which, as discussed below, can be very slow or also frozen. Relations with the dynamics of structural glasses have been also considered [10, 11]. One can expect that in real systems the effects of the velocity field, inducing motion around

(*) Present address: Department of Physics, Yoshida-south Campus, Kyoto University - Sakyo-ku, Kyoto, 606-8501 Japan.

local or extended defects, can be relevant. Our purpose here is to analyze the process of lamellar ordering taking into account the effects of hydrodynamics. We consider a model based on a Ginzburg-Landau free energy, where dynamics is described by convection-diffusion and Navier-Stokes equations [12]. Our results for two-dimensional systems show that, when hydrodynamical modes are effective (at sufficiently low viscosities), dynamical scaling holds with a complex dependence of characteristic lengths on time, analogous to that of systems with quenched disorder [13] not present here. An intermediate faster growth is followed by a slower logarithmic evolution at later times. The slowing-down of the dynamics is attributed to the formation of extended defects between domains of lamellae with different orientation, almost perpendicular to each other. Our simulations show that the same phenomenon occurs in three-dimensional systems. These results are not expected to depend on the specific model considered and could be relevant for a broad class of systems with lamellar order. We also verified that applied shear flows alleviate frustration giving power law growth at all times.

The model. – We consider the free-energy model [14, 15]

$$\mathcal{F}\{\varphi\} = \int \mathrm{d}^d x \left\{ \frac{a}{2}\varphi^2 + \frac{b}{4}\varphi^4 + \frac{\kappa}{2} \mid \nabla\varphi \mid^2 + \frac{c}{2}(\nabla^2\varphi)^2 \right\}, \tag{1}$$

where φ is the order parameter field representing the local concentration difference between the two components of the mixture. The parameters b and c have to be positive in order to ensure stability. For $a < 0$ and $\kappa > 0$, the two homogeneous phases with $\varphi = \pm\sqrt{-a/b}$ coexist. A negative κ favors the presence of interfaces and a transition into a lamellar phase can occur. In single-mode approximation, assuming a profile like $A \sin k_0 x$ for the direction transversal to the lamellae, one finds the transition ($|a| = b$) at $a \approx -1.11\kappa^2/c$, where $k_0 = \sqrt{-\kappa/2c}$, $A^2 = 4(1 + \kappa^2/4cb)/3$. The expression (1) can be also written for negative κ as $\mathcal{F}\{\varphi\} = \int \mathrm{d}^d x \{\frac{\tau}{2}\varphi^2 + \frac{b}{4}\varphi^4 + \frac{c}{2}[(\nabla^2 + k_0^2)\varphi]^2\}$, $\tau = a - ck_0^4$, and in this form it is generally used to describe di-block copolymers in the weak segregation limit [15].

The dynamical equations are [2]

$$\frac{\partial v_\alpha}{\partial t} + \boldsymbol{v}\cdot\boldsymbol{\nabla} v_\alpha = -\frac{1}{\varrho}\frac{\partial P_{\alpha\beta}}{\partial x_\beta} + \nu\nabla^2 v_\alpha\,, \tag{2}$$

$$\frac{\partial \varphi}{\partial t} + \boldsymbol{\nabla}\cdot(\varphi\boldsymbol{v}) = \Gamma\nabla^2\frac{\delta\mathcal{F}}{\delta\varphi}\,, \tag{3}$$

where v_α are the components of the velocity field, ϱ is the total density of the mixture and the incompressibility condition $\boldsymbol{\nabla}\cdot\boldsymbol{v} = 0$ is considered. ν is the kinematic viscosity and Γ is the mobility. The pressure tensor is the sum of the usual hydrodynamical part and of a tensor $P^{chem}_{\alpha\beta}$ depending on φ, with a functional form obtainable from the free energy containing off-diagonal terms, whose expression can be found in [12]. It can be shown that $\delta\mathcal{F}/\delta\varphi = 0$ implies $\partial_\alpha P^{chem}_{\alpha\beta} = 0$. The Laplacian in the r.h.s. of eq. (3) ensures the conservation of the order parameter. We will simulate these equations by using a finite-difference scheme for the convection-diffusion equation and a Lattice Boltzmann Method (LBM) for the Navier-Stokes equation. Advantages of this method [16] with respect to other LBM schemes for fluid mixtures are that spurious terms appearing in eq. (3) [17] are avoided and the numerical efficiency is increased. In $D = 3$ we used a parallel version of the LBM code which *fuses* the streaming and the collision processes to reduce bandwidth requirements [18]. Different numerical approaches have been also applied to lamellar systems. Among them we report studies using Dissipative Particle Dynamics [19], numerical solution of the amplitude equations

for fundamental modes [20], and LBM based on a force formulation [21]. The approach of this letter exploits the knowledge of the equilibrium properties of the system given a free energy.

We can summarize now what is known on the ordering properties of lamellar fluids. Previous two-dimensional studies of the full model (1)-(3) [12], without quantitative analysis due to the small size of the lattice considered (128^2), showed the relevance of hydrodynamics for obtaining well-ordered domains on the scale of the system simulated. More results exist for variants of the model (1) with long-range interactions, without hydrodynamics [22–24] or neglecting the inertial terms of the l.h.s. of eq. (2) [25]. Equation (3) without advection and with non-conserved order parameter, corresponding to the Swift-Hohenberg model for Raleigh-Bénard convection [26–30], has been also largely studied. Regimes with dynamical scaling have been found with the order parameter structure factor behaving as $C(\boldsymbol{k},t) \equiv \langle|\varphi_{\boldsymbol{k}}(t)|^2\rangle \sim t^z f[(k-k_0)t^z]$ with different values for the exponent z, $\varphi_{\boldsymbol{k}}(t)$ being the Fourier transform of $\varphi(\boldsymbol{x},t)$ [25, 27–33]. Slower evolution with frozen states and grain boundary pinning has been also observed [10, 29] for very deep quenches. In $D=3$, the few existing simulations have not considered dynamical scaling [21, 34].

Ordering dynamics. – We run our two-dimensional simulations on a 1024^2 lattice starting from disordered configurations. We fixed $|a|=b$ so that the minimum of the potential part of the free energy is at $\varphi=\pm1$. We checked on small systems (128^2) for different κ in the lamellar phase that the expected equilibrium state was reached. The value of c was fixed in such a way that the period is about 10 times the lattice spacing and $|a|=2\times10^{-4}$, $\kappa=-3\times|a|$, $c=3.8\times|a|$, $\Gamma=25$ for the cases presented. Details on the LBM part of the code can be found in [35].

After the quench, lamellae evolve until the equilibrium wavelength is locally reached. This part of the ordering does not depend on the value of viscosity. Later, however, the system continues to order only at sufficiently low viscosities ($\nu \lesssim 0.1$). Otherwise, local defects dominate [12] and, at times $t\sim3000$, the system results frozen in tangled configurations. An example of evolution at low viscosity ($\nu = 8.33\times10^{-3}$) is shown in fig. 1. Different kinds of

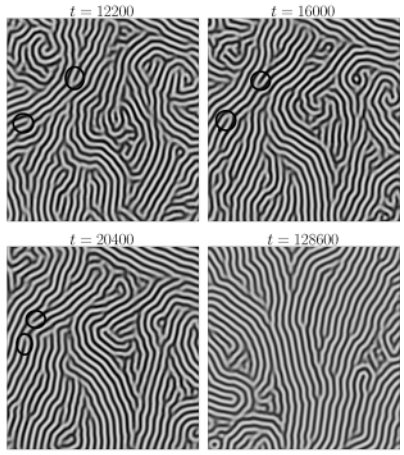

Fig. 1

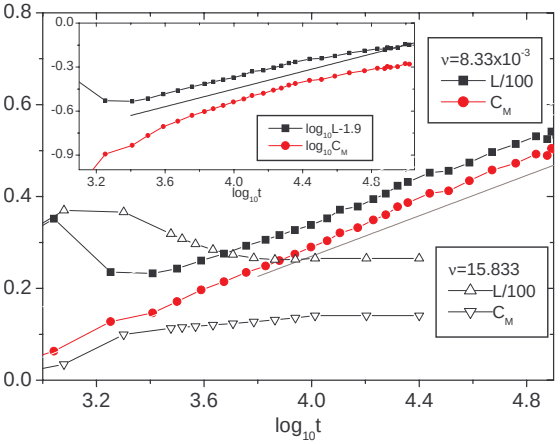

Fig. 2

Fig. 1 – Configurations at different times of a 256×256 portion of the lattice.

Fig. 2 – Time behavior of characteristic size L and $C_M \equiv C(k_M,t)$ on log-linear scales for two different viscosities. The straight line is a guide to the eye. In the inset the data for the case with lower viscosity are plotted on log-log scales; the straight line has slope 0.3.

defects can be observed. The annihilation of a couple of dislocations is highlighted. We have measured the relative velocity of the dislocations and we found it to be constant. At the last time of the figure the system can be observed to be ordered on larger scales.

A quantitative description of the ordering process comes from the analysis of the structure factor $C(\boldsymbol{k}, t)$. After spherical average we plotted $C(k, t)$ at different times. In the early regime, with $t \lesssim 3000$, $C(k, t)$ develops a maximum at a momentum k_M which decreases with time until the equilibrium value k_0 is reached. Then the peak of $C(k, t)$, remaining at k_0, continues to grow while the width decreases indicating an increase of order in the system. A characteristic length L for this process can be extracted from the structure factor in the usual way by measuring the full width δk of C at half-maximum and defining $L(t) = 2\pi/\delta k$. In the inset of fig. 2 we plotted $L(t)$ on log-log scale, calculated by averaging over 5 different runs. For more than one decade a behavior consistent with the power law $L \sim t^z$ can be observed with $z = 0.30 \pm 0.02$. The growth becomes slower at later times and we find $L \sim \ln t$ as the straight line in the main frame of fig. 2 suggests. We checked that the slowing-down cannot be attributed to finite-size effects (at the latest times considered, $L(t)$ is less than $1/10$ of the size of the system). For comparison, in fig. 2 the behavior of $L(t)$ for a quench with higher viscosity ($\nu = 15.833$), when the system becomes frozen, is also shown. $L(t)$ is almost constant from $\log t \sim 3.6$.

The behavior of L can be related to the role played in late-time dynamics by extended defects (grain boundaries) between domains of differently oriented lamellae. A decrease in the growing rate of L was observed at times $t \approx 25000$ when the average value of the angle between the normals of neighboring domains becomes close to 90°. Isolated grain boundaries can be shown to be stable defects in lamellar systems described by eq. (1) [10]. A quantitative description of ordering in lamellar systems can be obtained by considering the evolution equation for a single defect. The position x_{gb} of the grain boundary evolves according to $\dot{x}_{gb} = A\mathcal{C}^2(t) - B\cos(2k_0 x_{gb} + \phi)$, where $\mathcal{C}$ is the curvature of lamellae parallel to the boundary and A, B, ϕ are model-dependent parameters [10]. If one assumes that dynamical scaling is verified, a typical length can be defined as the inverse of curvature, and the previous equation implies a growth like $t^{1/3}$ until a critical value for curvature is reached. This analysis, elaborated for one single defect, suggests that in the ordering of a large system, in the absence of other processes and without hydrodynamics, defects will become pinned at a certain time with the system frozen in a configuration with many grain boundaries. In our case the velocity field helps the system in continuing the ordering process also at very late times but more slowly. We measured $L \sim \ln t$ which is the growth expected for systems with metastable states. An extension of the analytical arguments of [10, 36] in the presence of hydrodynamics is not available. However, it is interesting to observe that our simulations suggest an intermediate regime with a power law consistent with that of [10] followed by a logarithmic asymptotic growth, both results explainable as due to grain boundary dynamics.

We also considered three-dimensional systems. Simulations ranging from 64^3 to 512^3 lattices were performed: The largest grid required about 20 days of sustained computations, using a 8-CPU vector machine NEC SX6 and more than 32 GB of memory. While complete order was reached on 64^3 lattices, larger systems confirm the role of grain boundaries in lamellar ordering. An example is given in fig. 3, where a single grain boundary is shown: After $t \sim 10^7$ no clear 2D ordering was observed. On the 512^3 lattice we studied the behavior of $L(t)$, defined as in $D = 2$. After the formation of lamellae, the intermediate and late-time regimes were found shorter and it was not possible to deduce quantitative behaviors. However, the role of grain boundaries can be appreciated by looking, for example, at the configurations of fig. 4. Here the central horizontal sections of the system at $t = 600000$ and $t = 700000$ are shown. Many grain boundaries with three main orientations can be seen. After $t \sim 600000$, in correspondence of a sudden decrease observed in the growing rate of $L(t)$, the further

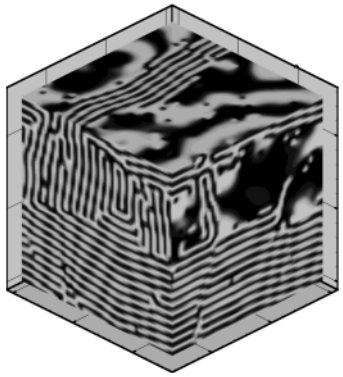

Fig. 3

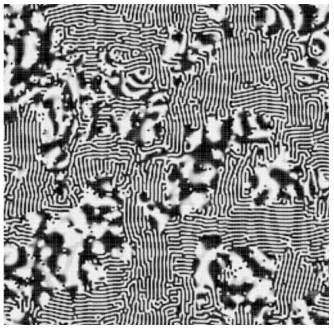

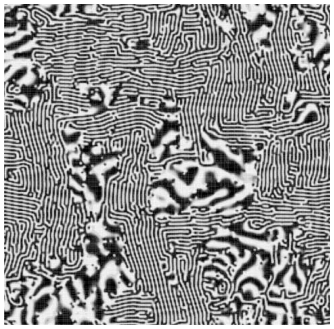

Fig. 4

Fig. 3 – Configuration of a 128^3 system at $t = 1000000$. The following parameters were used: $a = -b = -0.026$, $\kappa = -0.005$, $c = 0.0025$, $\Gamma = 0.25$, and $\nu = 0.1$.

Fig. 4 – The middle horizontal sections of a 512^3 systems at times $t = 600000$ and $t = 700000$. Parameters of this simulations are the same as in fig. 3. Observe how the vertical stripes in the central bottom part of the figures are distorted by the pressure of horizontal domains.

evolution of the system proceeds through the distortion of the grain boundaries existing at that time. This can be seen, for example, in the central bottom part of the configuration at $t = 700000$. Different domains, trying to increase their size, push themselves reciprocally, helped by the velocity field. This gives an unexpected late-time increase of curvature, also observed in $D = 2$. The role of hydrodynamics is important in this process: The system can reach a higher degree of order only by developing a strong velocity field which bends the existing flat grain boundaries. This will eventually bring later to a configuration with less defects. This picture is confirmed by the increase of kinetic energy observed at $t \sim 600000$.

Dynamical scaling. – In order to analyze dynamical scaling, together with $L(t)$, we also considered the behavior of the peak $C_M \equiv C(k_M, t)$ of the structure factor. In two-dimensional simulations, from fig. 2, one sees that C_M grows similarly to $L(t)$ but with a different rate. This suggests to consider scaling behavior in the general form $C(k,t) \sim L^\alpha f[(k - k_M)L]$ [37]. This differs from the usual expression considered in lamellar ordering ($C \sim t^z f[(k - k_M)t^z]$) for the introduction of α and the use of L even if not given by a power law. As illustrated in the inset of fig. 5, we evaluated $\alpha = 1.25 \pm 0.04$. Then, by using this value, we found, as shown in fig. 5, that rescaled structure factors overlap *at all times* after $t \sim 3000$ on a single curve, confirming our scaling assumption and suggesting an analogy with kinetic behavior in systems with quenched disorder. In Random Field Ising Models (RFIM), for example, diffusive growth changes over to logarithmic behavior but dynamical scaling holds at all times with the same scaling function as in standard Ising model [13]. Here, a similar scenario occurs but without quenched disorder. This is interesting also in relation with the existence of an equilibrium glass transition in systems with lamellar order [11].

Concerning the exponent α, its value is related to the compactness of domains and is $\alpha = D$ in asymptotic growth of binary mixtures, $\alpha = 0$ in early time regime when interfaces are forming [37]. Our results with $\alpha > 1$ show that the argument for $\alpha = 1$ based on the existence of one scaling dimension for 2D lamellar systems [27] does not hold in the presence of hydrodynamics. We found dynamical scaling also in 3D simulations but for a shorter time interval due to the limited size of the considered lattice.

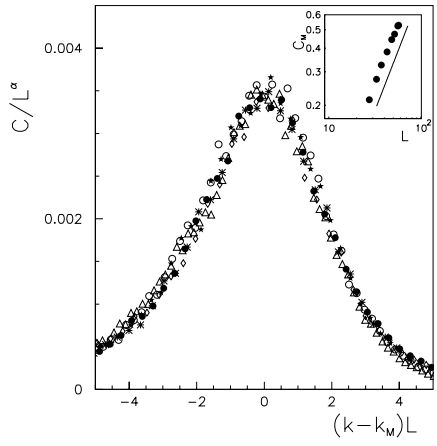

Fig. 5

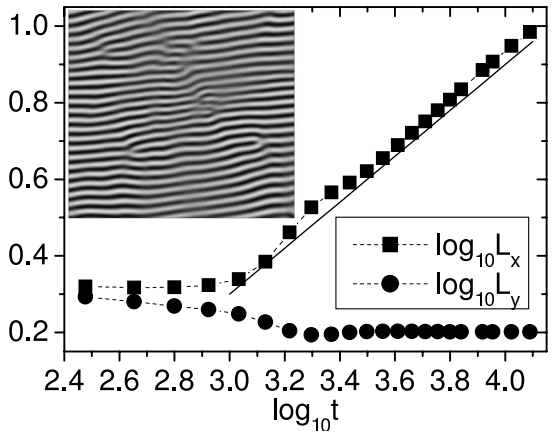

Fig. 6

Fig. 5 – Rescaled structure factors at different times. Data come from one of the runs in fig. 2 with $\nu = 0.00833$ (other runs with different initial configurations give same results). Symbols $\triangle$, $\circ$, $\star$, $\bullet$, $*$, $\diamond$ refer to times 4600, 14100, 40800, 61100, 78100, 123100, respectively. In the inset C_M is plotted on log-log scale as a function of L; the slope of the line is 1.25.

Fig. 6 – Evolution of L_x and L_y for $\dot{\gamma} = 10^{-4}$. The straight line has slope 0.6. At the latest times of the figure the system is almost completely ordered, as shown in the 200×200 portion of the inset.

Shear effects. – We also studied lamellar ordering in the presence of shear flow. Shear was applied with bounce-back conditions on rigid walls moving with velocity $\pm v_{wall}$ at the top and bottom of the simulation volume [35]. Ordering is favored since interfaces want to orientate with the flow [38]. Breaking and recombination of domains, induced by shear, make the elimination of topological defects faster [39]. As a result, logarithmic growth disappears and ordering occurs also asymptotically with power law behavior even in cases, at high viscosity, where without shear freezing would have been observed.

An example of this behavior ($\nu = 7.5$) is shown in fig. 6. Growth was measured by the quantities $L_\alpha = \int \mathrm{d}\boldsymbol{k} C(\boldsymbol{k},t) / \int \mathrm{d}\boldsymbol{k} |k_\alpha| C(\boldsymbol{k},t)$ ($\alpha = x, y$). L_x grows with exponent $z_x = 0.6$ while L_y relaxes to the equilibrium value. Similar results were found for other values of ν; a detailed exposition of our results with shear will appear elsewhere.

Conclusions. – To conclude, we have studied lamellar ordering in fluid mixtures with competitive interactions. At low viscosities, when hydrodynamic modes are effective, dynamical scaling holds in the form $C(\boldsymbol{k},t) \sim L^\alpha f[(k-k_M)L]$, where L is a characteristic length with complex behavior and logarithmic growth at late times. This scaling, similar to that found in systems with quenched disorder, is shown here for the first time in 2D systems with lamellar order. 3D simulations also show the relevance of grain boundaries defects for this dynamics. Shear flow removes extended defects giving power law behavior at all times.

* * *

We warmly thank F. Corberi, E. Orlandini, M. Zannetti and J. Yeomans for helpful discussions. We acknowledge support by MIUR (PRIN-2004).

REFERENCES

[1] See, *e.g.*, BRAY A. J., *Adv. Phys.*, **43** (1994) 357.
[2] See, *e.g.*, YEOMANS J. M., *Ann. Rev. Comput. Phys.*, **VII** (2000) 61.
[3] BATES F. S. and FREDRICKSON G., *Ann. Rev. Phys. Chem.*, **41** (1990) 525.
[4] GOMPPER G. and SCHICK M., *Phase Transitions and Critical Phenomena*,, Vol. **16** (Academic, New York) 1994.
[5] See, for example, DE GENNES P. G., *The Physics of Liquid Crystals* (Clarendon, Oxford) 1974.
[6] ROLAND C. and DESAI R. C., *Phys. Rev. B*, **42** (1990) 6658.
[7] KIVELSON D., KIVELSON S. A., ZHAO X., NUSSINOV Z. and TARJUS G., *Physica A*, **219** (1995) 27; GROUSSON M., KRAKOVIACK V., TARJUS G. and VIOT P., *Phys. Rev. E*, **66** (2002) 026126.
[8] GLOTZER S. C., DI MARZIO E. A. and MUTHUKUMAR M., *Phys. Rev. Lett.*, **74** (1995) 2034.
[9] CROSS M. C. and HOHENBERG P. C., *Rev. Mod. Phys.*, **65** (1993) 851.
[10] BOYER D. and VIÑALS J., *Phys. Rev. E*, **65** (2002) 046119.
[11] SCHMALIAN J. and WOLYNES P. G., *Phys. Rev. Lett.*, **85** (2000) 836; GROUSSON M., TARJUS G. and VIOT P., *Phys. Rev. Lett.*, **86** (2001) 3455.
[12] GONNELLA G., ORLANDINI E. and YEOMANS J. M., *Phys. Rev. Lett.*, **78** (1997) 1695; *Phys. Rev. E*, **58** (1998) 480.
[13] RAO M. and CHAKRABARTI A., *Phys. Rev. Lett.*, **71** (1993) 3501.
[14] BRAZOVSKII S. A., *Sov. Phys. JETP*, **41** (1975) 85.
[15] LEIBLER L., *Macromolecules*, **13** (1980) 1602; OHTA T. and KAWASAKI K., *Macromolecules*, **19** (1986) 2621; FREDRICKSON G. H. and HELFAND E., *J. Chem. Phys.*, **87** (1987) 697.
[16] Details about the method will appear elsewhere.
[17] SWIFT M. R., ORLANDINI E., OSBORN W. R. and YEOMANS J. M., *Phys. Rev. E*, **54** (1996) 5041.
[18] AMATI G. and MASSAIOLI F., *Proceedings of IBM ScicomP9, Bologna, Italy, 23-26 March 2004*, `http://www.spscicomp .org/cicomP9/Presentations/MassaioliAmatiScicomp09.pdf` (2004).
[19] GROOT R. D. and MADDEN T. J., *J. Chem. Phys.*, **108** (1998) 8713; GROOT R. D., MADDEN T. J. and TILDESLEY D. J., *J. Chem. Phys.*, **110** (1999) 9739; ZHANG K. and MANKE C. W., *Comp. Phys. Commun.*, **129** (2000) 275.
[20] YAMADA K., NONOMURA M. and OHTA T., *Macromolecules*, **37** (2004) 5762.
[21] GONZALEZ-SEGREDO N. and COVENEY P. V., *Europhys. Lett.*, **65** (2004) 795.
[22] LIU F. and GOLDENFELD N., *Phys. Rev. A*, **39** (1989) 4805.
[23] SHIWA Y., TANEIKE T. and YOKOJIMA Y., *Phys. Rev. Lett.*, **77** (1996) 4378.
[24] MAURITS N. M., ZVELINDOVSKY A. V., SEVINK G. I. A., VAN VLIMMEREN B. A. C. and FRAAIJE J. G. E. M., *J. Chem. Phys.*, **108** (1998) 9150.
[25] YOKOJIMA Y. and SHIWA Y., *Phys. Rev. E*, **65** (2002) 056308.
[26] SWIFT J. and HOHENBERG P. C., *Phys. Rev. A*, **15** (1977) 319.
[27] ELDER K. R., VIÑALS J. and GRANT M., *Phys. Rev. Lett.*, **68** (1992) 3024.
[28] CROSS M. C. and MEIRON D. I., *Phys. Rev. Lett.*, **75** (1995) 2152.
[29] HOU Q., SASA S. and GOLDENFELD N., *Physica A*, **239** (1997) 219.
[30] BOYER D. and VIÑALS J., *Phys. Rev. E*, **64** (2001) 050101(R).
[31] CHRISTENSEN J. J. and BRAY A. J., *Phys. Rev. E*, **58** (1998) 5364.
[32] QIAN H. and MAZENKO G. F., *Phys. Rev. E*, **67** (2003) 036102.
[33] HARRISON C. *et al.*, *Science*, **290** (2000) 1558; *Phys. Rev. E*, **66** (2002) 011706.
[34] NONOMURA M., YAMADA K. and OHTA T., *J. Phys. Condens. Matter*, **15** (2003) L423.
[35] XU AIGUO, GONNELLA G. and LAMURA A., *Phys. Rev. E*, **67** (2003) 056105.
[36] HUANG Z. F. and VIÑALS J., *Phys. Rev. E*, **71** (2005) 031501, preprint cond-mat/0411284.
[37] CONIGLIO A., RUGGIERO P. and ZANNETTI M., *Phys. Rev. E*, **50** (1994) 1046.
[38] See, *e.g.*, ONUKI A., *J. Phys. Condens. Matter*, **9** (1997) 6119.
[39] CORBERI F., GONNELLA G. and LAMURA A., *Phys. Rev. Lett.*, **83** (1999) 4057; **81** (1998) 3852.